FACULDADE DE ENGENHARIA DA UNIVERSIDADE DO PORTO

Analysis of Temporal Variations in Dermoscopy Images of Pigmented Skin Lesions by Machine Learning Techniques

Joana Raquel Martins Veiga

Mestrado Integrado em Engenharia Eletrotécnica e de Computadores

Supervisor: Prof. Doutor João Manuel R. S. Tavares

July 26, 2018

Resumo

O Melanoma tem-se vindo a revelar uma das maiores preocupações da sociedade, aquando de uma cuidada análise ao panorama oncológico global. Se por um lado a taxa de incidência deste tipo de cancro é bastante relevante, por outro o número de mortes que ainda causa é verdadeiramente alarmante. A vigilância frequente das lesões de pele e o estudo de diversos fatores relacionados com esta doença constituem-se como peças fundamentais de um diagnóstico precoce, traduzido numa mais rápida intervenção e consequente aumento da taxa de sobrevivência.

Neste sentido, a comunidade científica tem realizado diversos estudos que visam a melhoria dos sistemas assistidos por computador na tarefa de distinguir lesões malignas de benignas. Estes podem ser usados pelos médicos de modo a clarificar as caraterísticas da lesão, consolidando o diagnóstico cada vez mais fiável que pretendemos. Embora muitos destes estudos coloquem o seu foco na distinção das lesões, poucos são os que têm em conta a relevância da análise das variações temporais, ou seja, das diferenças que as lesões de pele apresentam ao longo do tempo.

O principal objetivo desta tese é o estudo da evolução das lesões pigmentadas de pele. Partindo de duas imagens da mesma lesão em diferentes momentos de avaliação procede-se à identificação de variações temporais que podem levar à intervenção do especialista. Estas possíveis alterações podem ser evidenciadas através de técnicas de processamento de imagem implementadas em MATLAB e podem revelar-se uma preciosa ajuda para o especialista na hora de tomar uma decisão. Este trabalho aborda os cinco passos principais que são o pré processamento, a segmentação, a extração de atributos, a seleção de atributos e a classificação. Os resultados obtidos baseiam-se no uso de diversos descritores em três diferentes cenários que incluem uma primeira análise apenas com as alterações, a segunda com descritores referentes ao segundo momento de avaliação da lesão e a terceira tendo em conta ambos os cenários.

Palavras chave: Variações Temporais, Lesões de pele, Segmentação, Extração de caraterísticas, Seleção de caraterísticas

Abstract

Melanoma is a worldwide concern due to its thousands of cases and number of deaths from this cancer. Frequent surveillance of skin lesions and the study of several factors associated with this disease can lead to an early diagnosis leading to rapid intervention and increasing the survival rate.

In this sense, the scientific community has carried out several studies aiming a performance improvement of computer-assisted systems in the task of distinguishing between malignant and benign lesions. These can be used by physicians in order to clarify the characteristics of the lesions, reinforcing an increasingly reliable diagnosis. Although several of these studies focus on the distinction of lesions, there are not so many that take into account the relevance of the analysis of temporal variations, that is, the differences that the skin lesions present over time.

The main goal of this thesis is the study of the evolution of pigmented skin lesions. Starting from two images of the same lesion at different moments of evaluation, that is the identification of changes that may lead to the intervention of the specialist. These possible alterations may be evidenced through image processing techniques implemented using MATLAB which may help the physician to make a decision. This work addresses five main steps in image processing namely pre-processing, segmentation, feature extraction, feature selection and classification. The obtained results are based on the use of several descriptors in three different scenarios which include a first analysis with only the alterations, the second with the descriptors referring to the second evaluation moment and the third taking into account these two mentioned scenarios.

Key words: Temporal Variations, Skin lesions, Segmentation, Feature extraction, Feature Selection

Agradecimentos

Agradeço ao Professor João Tavares pela disponibilidade constante e orientação no decorrer desta tese. Ao Dr. Jorge Rozeira pelas imagens usadas no trabalho e por toda a sua preocupação e apoio. Aos meus pais e irmão porque são a razão de eu continuar de pé ao fim destes cinco anos. Ao Orfeão Universitário do Porto por me ter dado bons amigos, boas viagens, boas aventuras e boas gargalhadas. Aos que são meus amigos.

Joana Veiga

"Not everything that can be counted counts
and not everything that counts can be counted"

William Bruce Cameron

Contents

List of Figures

List of Tables

Abbreviations

PSL	Pigmented Skin Lesion
BCC	Basal Cell Carcinoma
SCC	Squamous Cell Carcinoma
XP	Xeroderma Pigmentosum
CAD	Computer-Aided Diagnosis
GLA	Generalized Lloyd algorithm
PGF	Peer Group Filter
RGB	Red Green Blue
KL	Karhunen-Love
ROI	Region of Interest
GLCM	Grey Level Co-occurence Matrix
ANN	Artificial Neural Network
MLP	Multilayer Perceptron
SVM	Support Vector Machine
PCA	Pearson's Correlation Attribute
UV	Ultraviolet
DNA	Deoxyribonucleic Acid
AI	Artificial Inteligence
FCM	Fuzzy C Means Algorithm
PCM	Possibilistic C Means Algorithm
HCM	Hierarchical C Means Algorithm
FHNN	Fuzzy Hopfield Neural Network
GVF	Gradient Vector Flow
HSV	Hue Saturation Value
TP	True Positive
TN	True Negative
FP	False Positive
FN	False Negative
KNN	K-nearest Neighbour
PCA	Pearson's Correlation Attribute
NB	Naive Bayes

Chapter 1

Introduction

1.1 Motivation

Each year more people are diagnosed with skin cancer all over the world. The large incidence in population is causing a huge concern to the scientific community, which leads the development of multiple studies related to diagnose this type of cancer.

Melanoma is the skin cancer that has the highest mortality rate. In U.S it is estimated 91,000 new cases and 9, 000 deaths from melanoma during this year [44]. These statistics motivate an early diagnosis in order to reduce mortality. However, in early stages of this cancer, it becomes particularly difficult to distinguish between benign and malignant pigmented skin lesions. Thus this task may depend in part on the professional's experience resulting in different evaluations for the same lesion.

Although many skin lesions never present any problem, frequent surveillance is necessary to ensure a faster intervention in the event of any changes that may predict the development of melanoma. It is important to compare the lesions over time given their possible alteration and evolution that justify some attention and a diagnostic adjustment. One of the most relevant imaging techniques for pigmented skin lesions diagnosis is dermoscopy, a non-invasive technique that allows a better visualization of skin details not visible by naked eye [23]. This practice improves diagnostic accuracy and assists clinicians in detecting early stage melanoma that often gives an excellent prognosis to the patient when surgically removed.

Therefore computer-aided systems are becoming more important in this field due to the challenging task of discriminate benign from malignant skin lesions. These systems can process several images and are intended to make a decision based on the diagnosis achieved by the processing of the images which will reduce the dependency on the experience of the dermatologist and the time consumed in the visual interpretation of each lesion.

1.2 Objectives and methodology

The main goal of this thesis is the study of the evolution of pigmented skin lesions. Starting from two images of the same lesion at different moments of evaluation, that is the identification of changes that may lead to the intervention of the specialist. These possible alterations may be evidenced through image processing techniques and may help the physician to make a decision.

The first step was to conduct a literature review of this subject allowing the identification of the required steps to develop this study. The knowledge of the application of different used methods in pre-processing, segmentation, feature extraction, feature selection and classification provide a comparison of their performance for different situations. This review intends to find the best solution to the initial problem taking into account the results obtained for each situation and technique already studied.

After this initial task, all steps mentioned above will be performed based on methods commonly used in the literature. Thus, all images will be preprocessed in order to prepare them for the next step (segmentation) reducing and smoothing undesired artifacts. The segmentation step allows to define the region of the skin lesion which will be crucial and determinant in feature extraction from the lesion's domain. After the features are extracted they will be analyzed in order to proceed to its classification (malignant or benign) presenting 3 scenarios: classification taking into account the variations of the lesion between two moments; classification with the features extracted from the lesion in the second moment and the classification according to the differences observed in features and the measurements from the second moment of evaluation. Finally, it is intended to prove the efficacy of a skin lesion classification system using temporal analysis with the possible changes evidenced by each feature.

Therefore, this project aims to provide information that can be useful to assist the physicians in the diagnosis of skin cancer.

1.3 Document structure

This thesis is divided into four chapters, excluding the introduction, corresponding to the four phases of the project development:

- **Chapter 2: Literature Review** — This chapter presents some literature used for the development of this project. In addition to a brief introduction to skin lesions, risk factors and diagnostic methods used by dermatologists, this chapter is also dedicated to the description of recent work developed for each CAD system step.

- **Chapter 3: Methodology** — Based on the presented literature, this chapter describes the adopted procedure in the course of this thesis. The implementation of all methods and techniques will be explained in detail in order to a better understand of the developed work.

- **Chapter 4: Results and Discussion** — In this chapter will be presented the obtained results with the used procedure and its subsequent discussion. In addition it also explains the main problems faced during the implementation of the methods and the found solutions.
- **Chapter 5: Conclusions** — After the performed work, this chapter presents the final comments, taking into account the initial objectives and the achieved results. Some improvements and strategies will be proposed for possible future work.

Chapter 2

Literature Review

This chapter covers most of the main literature related to this subject and were the basis of the development of this work. The following sections present several studies to achieve the purpose of this thesis.

Firstly, it is presented a brief introduction to pigmented skin lesions, highlighting the various types of skin cancer and associated risk factors, the analysis method of dermoscopy used in clinical practice and some criteria followed by physicians in the diagnosis of melanocytic lesions. In addition, the most frequently used approaches and techniques are presented for each step involved in assessing a diagnosis using a CAD system specifically pre-processing, segmentation, feature extraction, feature selection and classification.

2.1 Pigmented skin lesions

2.1.1 Skin lesions

Skin cancer occurs when normal skin cells multiply without control. Pigmented Skin Lesions (PSL) are examples of these growths that appear on the skin surface easily distinguished by the color from the rest of the skin. These lesions include malignant and beningn forms.

There are three major types of skin cancer: basal cell carcinoma (BCC), squamous cell carcinoma (SCC) and melanoma. Although BCC and SCC are more common, melanoma is the deadliest one.

There are several risk factors that affect the chance of getting melanoma skin cancer. However having them does not mean that a person will develop the disease. Knowing the risk factors associated to melanoma is quite important since it is often possible to reduce the probability of having it and to do things that help detect it as early as possible. The most important risks are presented below [44]:

- **Ultraviolet (UV) light exposure** — it is a considerable risk factor for most melanomas since UV rays can influence skin cell growth by damaging its DNA. These rays includes those that came from the sun and other sources like tanning beds and sun lumps;

- **Moles** — having many moles indicate higher probability of developing melanoma. Although the possibility of a mole becomes cancer be very low, a lot of large and irregular moles may increase this probability;
- **Fair skin, freckling, and light hair** — those people who have these factors are at increased risk. It is more probably a white person develops a melanoma than an african american;
- **Family history** — shared lifestyles that may indicate similar sun exposure, a tendency to have fair skin, and certain genetic mutations are factors common to families. Thus around 10% people who develop this deasease have family history;
- **Personal history** — people who have melanoma or other skin cancers history are at a increased risk of getting this disease;
- **Weake immune system** — all diseases and situations that weaken people's immune system put them at a higher risk of developing many types of skin cancer like melanoma;
- **Being older** — most melanomas occur in older people;
- **Being male** — men have a higher rate of getting melanoma;
- **Xeroderma pigmentosum (XP)** — it is a condition that avoid the repair of DNA of skin cells. XP is inherited and people who have it are at an increased risk of getting skin cancer at a younger age on sun-exposed body areas;

Given the presented risks there are many things that people can look for in the prevention and early diagnosis of melanoma. However the task of detecting malignant or potentially malignant skin lesions can be difficult even for dermatologists. That is why they often make use of non-invasive imaging techniques in order to collect an image that allows a better structure identification of a certain lesion without having to remove it surgically. For example macroscopic and dermoscopic images are obtained using common digital cameras and a dermatoscope respectively allowing more detailed visualization of the lesion. As a non-invasive technique it is also used for follow-up the lesions over time in order to act early if any changes that may predict melanoma appear.

2.1.2 Dermoscopy image analysis

Dermoscopy is a non-invasive technique that enlarges skin structures using an optical lens (a dermoscope) and liquid immersion in order to help diagnosing pigmented skin lesions giving specialists confidence in determining the lesion [29]. Furthermore this method can improve diagnosis sensivity since it provides dermoscopy images that can help to obtain an improved analysis [11].

The combination of dermoscopy and computer aided diagnosis (CAD) is the target of much reasearch that tries to reduce time loss and variations inherent to the observer [13] [14]. Hence there are fundamental steps recognized in many computational systems which cover image preprocessing, segmentation, feature extraction and selection and classification. One of the reasons

why border detection is made by these systems is based on the difficulty that the human eye has in perceiving minor color and shape changes allowing a better representation of the lesion and consequently an improved extraction of its features. However this task only becomes less complex when pre-processing is completed, eliminating several factors that make it difficult.

2.1.3 Differential diagnosis

Dermoscopy images help to decide whether or not the lesions are melanocytic. If classified as such the next step is to determine whether there are malignant or benign. In this phase there are four commonly used approachs to evaluate the skin lesion: the seven-point checklist, the Menzies method, the pattern analysis or the ABCDE rule [8].

The pattern analysis is a method often used by experienced dermatologists once it requires knowledge and recognition of the global and local patterns of the lesions in order to distinct between benign and malignant growths [8]. There are some feautures that help in this decision like the color appearance, the architectural order, the pattern symmetry and the homogeneity (CASH) of them. In the case of benign melanocytic lesions it is usual the presence of few colors, an architectural order, a pattern symmetry and homogeneity. For malignant melanoma it is often seen the opposite like many colors, a much architectural disorder, an evident pattern assymetry and heterogeneity [8].

The seven-point checklist is based on the attributed scores to 3 major and 4 minor criteria (Table 2.1). For melanoma diagnosis it is requested at least a score of 3 [8].

Table 2.1: The 7-point checklist

Criteria	**7-point score**
Major criteria	
Atypical pigment network	2
Gray-blue areas	2
Atypical vascular pattern	2
Minor criteria	
Irregular streaks	1
Irregular pigmentation	1
Irregular dots/globules	1
Regression pattern	1

The Menzies method is based in negative and positive features which can be observed in table 2.2. To diagnose melanoma must not be found both of the negative features and be found at least one positive feature [8].

The ABCDE rule is one of the starting points for the classification of melanomas and it emerged as an aid to early diagnosis based on a simple mnemonic easily used by everyone. It includes five parameters that can be applied to the lesions (Asymmetry, Border, Color, Diameter and Evolution or Evolving). In the case of melanoma, the irregularity and asymmetry of form, the difficulty in delimiting the lesion, the presence of more than one color or an uneven distribution of

Table 2.2: The Menzies method [49]

Negative features
Point and axial symmetry of Pigmentation Pattern
Single Color
Positive features
Blue-White Veil
Multiple Brown Dots
Pseudopods
Radial streaming
Scar-like Depigmentation
Peripheral Black Dots/Globules
Multiple (Five to Six) Colors
Multiple Blue-Gray Dots
Broadened Network

it and a diameter of more than 6mm are frequently verified and scored as shown in table 2.3. Regarding the *E* parameter there are studies that defend the importance of evolving pigmented lesions in the progression of melanoma and others that only focus on the analysis of possible changes in a given time, relative to the parameteres mentioned above.

2.2 Pre-processing

Pre-processing is an essential step often related to the efficiency of CAD systems in pigmented skin lesions analysis. It is proposed that the images used by these systems are prepared for the following step (segmentation) by enhancing the contrast, correcting illumination and removing unwanted artifacts. For example, hairs, ink markings, dermoscopic gel, air bubbles, uneven illumination and black frames may influence the accuracy of the segmentation step. Thus, in order to improve this procedure, there are many studies which are particularly interested in this step.

One of the used techniques is the application of filters that soften the image, such as median filters [12] [15], Gaussian filters [37] and anisotropic filters [10] as shown in figure **??**.

The median filter with an appropriate size mask may reduce the influence of undesired artifacts in the segmentation step [15]. Celebi et al. [12] presented the comparison between the Peer Group Filter (PGF) and the median filter and conclude that median filter shows a better performance in

Table 2.3: Weight score of the ABCD rule features

	Score	Weight factor
Assymmetry	0-2	1.3
Border	0-8	0.1
Color	1-6	0.5
Diameter	1-5	0.5

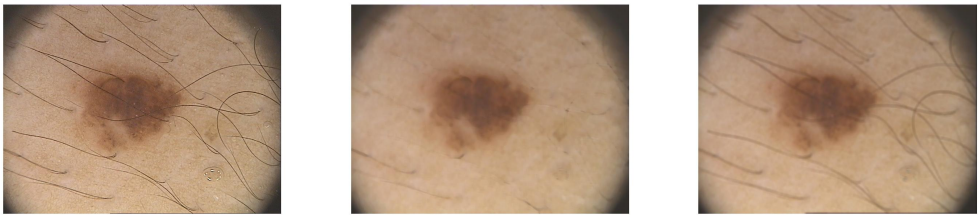

(a) (b) (c)

Figure 2.1: Image after applying median and gaussian filter: a) Original Image, (b) median filter and c) gaussian filter

reducing hairs and air bubbles. There are also other techniques related to image contrast enhancement. In [2] it is proposed an optimal solution adapted to human perception using components of *CIECAM02* color appearance model.

During the digitalization process of dermoscopy images it is frequent the appearance of black frames. Abbas, Celebi and Fondón [2] propose a method based on row by row image scanning that computes the darkness of a pixel. This procedure is repeated in each three main directions and concludes that a row is part of the black frame if it has 60% black pixels.

Also within the scope of this initial step there are inpainting techniques to fill parts of the image data after hair removal process in order to overcome this occlusion problem and improve the ROI perception [22]. These can be very interesting because improve this step performance and give physicians a clearer view of the lesion they want to analyze.

A color image obtained by non-invasive techniques contains thousands of colors. Thus a color quantization in pre-processing step can help color image segmentation. In [12] is studied the application of a modified Generalized Lloyd Algorithm (GLA) to quantize the pixel colors and are presented the main problems that may arise from it.

The color space transformation is also a used technique due to the simplicity and convenience of a scalar image. The input RGB image is converted using different methods like retainig only the blue channel (lesion may become more proeminent on this channel), applying the Karhunen-Love (KL) transformation and retaining the channel with the highest variance and applying the luminance tranformation [21].

2.3 Segmentation

After the image pre-processing, the following step is segmentation, a crucial step that allows to delineate the region of interest. It is intended that the lesion region be correctly distinguished from the rest of the surrounding skin so that their characteristics are extracted allowing a correct classification. However, this task is very complex because of the lesion variety in shape, size, texture and colors. Therefore, there are several methods that aim more and more a greater precision of this task, since its result is determinant to the diagnosis accuracy due to the influence in the following steps. The introduction of CAD systems has become crucial in resolving these problematics and

in minimizing the intra and inter operator dependencies. Therefore many times this step is done manually to build an increasingly reliable ground truth [23].

There are several segmentations methods commonly classified as thresholding-based, region-based and edge-based. Beyond these there are also methods based on artificial intelligence (AI) and active contours. Once this is a very important step it can be found in the literature multiple comparisons between different methods [43], which help to perceive the differences between each of them.

One of the most used methods of image segmentation is the thresholding method due to its simplicity and fast implementation. This technique uses the histogram of the input images, corresponding to the possible levels of the intensity, and selects some values to separate the region of interest (ROI)[26]. Celebi et al. [17] also present an approach provided by an ensemble of thresholding methods. Therefore is possible to explore the peculiarities of the participating methods, this fusion intends to arrive to the best decision based on multiple comparisons of different thresholding methods. It also can be seen that different image characteristics determine different methods.

The edge-based segmentation detects and links edge pixels to form contours based on the changes in intensity of the pixels. This method is very interesting because it reduces the amount of data to be processed and preserve structural information about the lesion boundaries [9]. The edge detector that presents better results compared to others was developed by Canny and was applied in different studies using skin lesion images [20, 6].

In the case of region-based approaches there are several methods that group similar nearby pixels into a larger region according to the growing criterion as the case of the algorithm used by Celebi et al. [15]. Starting with a set of "seed" points, the region grows by appending to each of these points neighbour pixels that have identical properties. These methods may be preferable for noisy images since their edges are difficult to detect.

Other methods include AI and are based for example on clustering techniques[46]. Clustering algorithms involve a process of grouping samples (clusters) in which objects are identical using a predefined criteria to partition. A comparison of six clustering methods (Fuzzy C Means Algorithm (FCM), Possibilistic C Means Algorithm (PCM), Hierarchical C Means Algorithm (HCM), Fuzzy Hopfield Neural Network method (FHNN method), Regression Neural Network and Adaline Neural Network) with the manually segmented image shows that Hierarchical C Means algorithm (Fuzzy) provides better results [46].

Active contour methods also known as snake methods cover among others deformable models [31], gradient [53] and level set based methods [43]. A deformable model may be an interesting technique for image segmentation in medical image processing and analysis. These algorithms allow to evolve from an initial curve to the lesion's boundary applying a proper speed function and can be classified as parametric or geometric based on the tracking approach of curve evolution. In [31] is adopted the geometric model due to more simply computations since it is not necessary to track the movement of each curve point. A gradient based method attempt to find the skin lesion boundary with the gradient intensity observed in the image. The gradient vector

flow (GVF) appears as an alternative to the traditional snakes which have problems related to the initialization and poor convergency to the boundary [52]. The main differences introduced are in the formulation of the snake that is based directly from a force balance condition instead of a variational formulation and in the replacement of the negative potencial force. From the gray-level or the binary edge map of the skin lesion image, the GVF is computed as a difusion of its gradient vectors. Level set based methods try to minimize a contour's energy as a sum of internal and external energies [26].

2.4 Feature extraction

In order to develop a reliable CAD system that is capable of responding to the initial problem and distinguishing the different diagnoses of the lesions such as a dermatologist, the extraction of features becomes significant for the lesion characterization. These features follow a pattern where they are measurable and have high sensitivity [33] and can be divided into groups: shape features, color features and texture features.

2.4.1 Shape features

There are several features of this group that allow analyzing the lesion in terms of asymmetry, edges and diameter, that is, rules A, B and D from ABCDE rule. Since lesions with asymmetric shape and irregular borders are largely related to malignant lesions, these features have potential for the final goal. In the literature are presented several features such as area and perimeter [32], aspect ratio [16], compactness [16], assymetry index [36, 16], border irregularity [36], extent and solidy ratio [32].

Area (A) is a simple feature that indicates the relative size of the lesion and is given by the number of pixels inside ROI, ie inside lesion's border and perimeter (p) is given by the number of pixels that constitutes that border.

Aspect ratio is determined dividing the width by the height of the minimum rectangle that bounds the lesion region also known as bounding box ratio [32]. This feature is achievable by scanning the image and finding the lowest and the highest value to the row and column of the ROI.

Compactness (C) is defined as the ratio of the lesion's area to the area of a circle with the same perimeter [36] and is given by the equation 2.1 using the lesion area and perimeter.

$$C = \frac{p^2}{4\pi A} \tag{2.1}$$

Assymetry index gives a quantitative measure of the lesion assymetry [16, 36]. First, is calculated according to equation 2.2 the orientation of the lesion major axis

$$\theta = \frac{1}{2} tan^{-1}\left(\frac{2\mu_{11}}{\mu_{20} - \mu_{02}}\right) \tag{2.2}$$

where μ_{11}, μ_{20} and μ_{02} represent the standard moment, quadratic moment according to the horizontal Cartesian axis and quadratic moment according to the vertical Cartesian axis. Then is calculated two assymetry measures A_1 and A_2 using A_x and A_y obtained after the lesion's θ clockwise rotation. The lesion is hypothetically folded about the x and y axis resulting an area difference between the overlapping folds A_x and A_y respectively (equations 2.3 and 2.4).

$$A_1 = \frac{min(A_x, A_y)}{A} * 100\% \tag{2.3}$$

$$A_2 = \frac{A_x + A_y}{A} * 100\% \tag{2.4}$$

The border irregularity depends on edge precision and it can be measured calculating the fractal dimension using the box counting algorithm [36]. The first step is to divide the original image into a $m \cdot m$ pixel image which then is divided into cells of $s \cdot s$ resulting a dilatation ratio (k) given by m/s. Thus it can be calculated the number of cells (n) that contain a portion of the edge using equation 2.5.

$$d_{frac} = \frac{log(n)}{log(k)} \tag{2.5}$$

There are other ratios equally present and important in literature such as solidity ratio that is defined as the division of the skin lesion area by the area of the convex hull of the lesion boundary.

Statistical moments are also often used to describe shape since irregular shapes are often related to larger moments [1]. Thus, Hu [28] introduced a general approach that later Flusser and Suk [24] developed to invariance using general affine transformations. The equation 2.6 defines the $p+q$th order moment $M_{p,q}$ of a density distribution function $f(x,y)$.

$$M_{p,q} = \int_{-\infty}^{+\infty} \int_{-\infty}^{+\infty} x^p y^p f(x,y) dx dy \tag{2.6}$$

Starting from this equation the invariant features can be achieved using central moments once moments may vary when $f(x,y)$ changes by scaling and rotating:

$$\mu_{pq} = \int_{-\infty}^{+\infty} \int_{-\infty}^{+\infty} (x - x_c)^p (y - y_c)^q f(x,y) dx dy \tag{2.7}$$

where x_c and y_c represents the centroid coordinates of the image $f(x,y)$.

Once the centroid moments that are calculated using the centroid of the image (equation 2.7) are equivalent to the calculation presented by equation 2.6 whose center has been shifted to centroid of the image it can be concluded that the central moments are invariant to translations.

In order to obtain feature metrics that are rotation-, translation- and scaling invariant is only required to normalize those moments defined as

$$\eta_{pq} = \frac{\mu_{pq}}{\mu_{0,0}^{\gamma}} \tag{2.8}$$

where $p+q \geq 2$. Thus, Hu can delineate seven moment invariants ϕ_1 through $\phi 7$ defined as

$$\begin{aligned}
\phi_1 &= \eta_{2,0} + \eta_{0,2} \\
\phi_2 &= (\eta_{2,0} - \eta_{0,2})^2 + 4\eta_{1,1}^2 \\
\phi_3 &= (\eta_{3,0} - 3\eta_{1,2})^2 + (3\eta_{2,1} - \eta_{0,3})^2 \\
\phi_4 &= (\eta_{3,0} + \eta_{1,2})^2 + (\eta_{2,1} + \eta_{0,3})^2 \\
\phi_5 &= (\eta_{3,0} - 3\eta_{1,2})(\eta_{3,0} + \eta_{1,2}) \left[(\eta_{3,0} + \eta_{1,2})^2 - 3(\eta_{2,1} + \eta_{0,3})^2\right] \\
&\quad + (3\eta_{2,1} - \eta_{0,3})(\eta_{0,3} + \eta_{2,1}) \left[3(\eta_{1,2} + \eta_{3,0})^2 - (\eta_{2,1} + \eta_{0,3})^2\right] \\
\phi_6 &= (\eta_{2,0} - \eta_{0,2}) \left[(\eta_{1,2} + \eta_{3,0})^2 - (\eta_{2,1} + \eta_{0,3})^2\right] \\
\phi_7 &= (3\eta_{2,1} - \eta_{0,3})(\eta_{1,2} + \eta_{3,0}) \left[(\eta_{1,2} + \eta_{0,3})^2 - 3(\eta_{2,1} + \eta_{0,3})^2\right] \\
&\quad + (3\eta_{2,1} - \eta_{0,3})(\eta_{2,1} + \eta_{0,3}) \left[3(\eta_{1,2} + \eta_{3,0})^2 - (\eta_{2,1} + \eta_{0,3})^2\right]
\end{aligned} \tag{2.9}$$

2.4.2 Color features

These features are intended to quantify the color variation in the lesion and can be very helpful to classify the lesions. The dermoscopy images have usually their color information stored in RGB components, a color space that represents the values three channels (red, green and blue). However, there are several other color models well-accepted in the digital image processing such as CIELAB, CIELUV, CIEXY, CMY, CMYK, HSL, HSV and others [29]. Although the images were originally obtained with the RGB components, this color space is often converted to another one in order to separate lightness information from chromaticity. This first have some disadvantages such as the high correlation between channels and the perceptual non-uniformity [48] and the separation mentioned above can decreases the distortions related to lightness [32].

HSV, $I1/2/3$ and $CIEL*u*v$ are examples of color spaces that do decoupling of chrominance and luminance. HSV color space represents the hue, saturation and value channels and this model is easily achievable from the RGB model [39] using the following conversion equations:

$$\begin{aligned}
V &= max(R,G,B) \\
S &= \begin{cases} [V - min(R,G,B)]/V, & \text{if V} \neq 0 \\ 0, & \text{if V} = 0 \end{cases} \\
H &= \begin{cases} 60(G-B)/[V - min(R,G,B)], & \text{if V} = R \\ 120 + 60(B-R)/[V - min(R,G,B)], & \text{if V} = G \\ 240 + 60(R-G)/[V - min(R,G,B)], & \text{if V} = B \end{cases} \\
H &= H + 360, \text{if H} < 0
\end{aligned} \tag{2.10}$$

The separation of each channel is given by $H = H/2$, $S = 255S$ and $V = 255V$.

$CIEL*u*v$ is one of the models proposed by the International Commission on Illumination (CIE - Commission Internationale de I'Eclairage) with the purpose of providing a perceptually

uniform colour space since the Euclidean distance between two colours is correlated with the human visual perception. This colour space normalizes its values by the subtraction of the white colour point [48]. The tranformation equations from $CIEXYZ$ to $CIEL*u*v$ are presented below [48]:

$$\begin{aligned}
L &= \begin{cases} 116\left(\frac{Y}{Y_n}\right)^{1/3}, & \text{for Y} > 0.008856 \\ \frac{903.3Y}{Y_n}, & \text{for Y} \leq 0.008856 \end{cases} \\
u &= 13L(u' - u_n), \\
v &= 13L(v' - v_n), \\
u' &= \frac{4X}{X + 15Y + 3Z}, \\
v' &= \frac{9Y}{X + 15Y + 3Z}, \\
u_n &= \frac{4X_n}{X_n + 15Y_n + 3Z_n}, \\
v_n &= \frac{9Y_n}{X_n + 15Y_n + 3Z_n},
\end{aligned} \tag{2.11}$$

where $0 \leq L \leq 100$, $-134 \leq u \leq 220$ and $-140 \leq v \leq 122$. The separation of each channel is given by $L = \frac{L*255}{100}$, $u = \frac{255}{354}(u + 134)$ and $v = \frac{255}{262}(v + 140)$ [39].

The most frequent colour features extracted from these channels are the mean 2.12, standard deviation 2.13, skewness 2.14 and variance 2.15 values of each channel [45]

$$\mu = \frac{1}{N}\sum_{j=1}^{N} p_j \tag{2.12}$$

$$\sigma = \sqrt{\frac{1}{N}\sum_{j=1}^{N}(p_j - \mu)^2} \tag{2.13}$$

$$S = \sqrt[3]{\frac{1}{N}\left(\sum_{j=1}^{N}(p_j - \mu)^3\right)} \tag{2.14}$$

$$V = \frac{1}{N}\sum_{j=1}^{N}(p_j - \mu)^2 \tag{2.15}$$

where j is the jth pixel of a color channel p of an image with N pixels in a color space. Beyond these it can be included the Euclidean distances that are calculated by the difference between a chromaticity and the mean chromaticity of the skin lesion using the chromaticity coordinates u^*

and v^* [32]. The equation 2.16 represents this calculation

$$d = \sqrt{(u^* - u_1^*)^2 + (v^* - v_1^*)^2} \tag{2.16}$$

where u_1^* and v_1^* are the mean of u^* and v^* being that the skin lesion chromatic geometric centroid is (u_1^*, v_1^*). Then it can be defined the mean and standard deviation of d. This whole process can be done not only for the skin lesion but also for the surrounding healthy skin increasing the number of extracted features.

2.4.3 Texture features

Texture is one characteristic that plays an important role in human visual perception of skin lesions and is very helpful for their recognition and interpretation. Therefore, texture features can be quite important when extracting features that allow to distinguish between malignant and benign lesions. These features include four main approaches: statistical-, structural-, model- and filter-based approaches [50]. One of the most well-known method to extract texture features is the spatial greylevel co-occurence matrix (GLCM) [27], a statistical-based descriptor that measures the probability of two image pixels have a specific grey level given a fixed vector. This matrix is the starting point to compute several features such as energy, contrast, entropy, correlation, homogeneity, inverse difference, mean and standard deviation. These features are choosen due to their robustness to linear shifts in the intensity.

Model-based texture methods include, among others, fractal models [41], autoregressive models [35] and random field models [18]. The fractal dimension is one of the most important measurements in fractal models and there are different methods to estimate it such the walking-divided method, the box-counting method, the robust fractal estimator, among others [3]. The principle of these methods is based on the texture segmentation of images that be useful to quantify the irregularity and self-similarity of the image's fractals given by fractal dimension variations.

2.5 Feature selection

The feature selection step allows to reduce the dimensionality of the feature space by removing irrelevant and/or redundant features. Therefore, this stage of pre-processing is done before proceeding to the classification of the lesions improving the accuracy rate and reducing not only the feature extraction time, but also the training and testing time and the inherent complexity of the classifier [16].

In [19] are presented four main steps that can divide the feature selection process:

1. a generation procedure – a search procedure that generates subsets of features for evaluation;

2. an evaluation function – to evaluate the subset produced. The resultant measure is iteratively compared with the previous best, replacing it if it be found a better one;
3. a stopping criterion – to decide when to stop avoiding a exhaustive search;
4. a validation procedure – to check the validity of the subset.

For the first step there are several search algorithms that allow to identify a feature subset for evaluation namely best-first, ranker, incremental stepwise and random. Other examples include exhaustive search and embedded methods such as decision trees algorithms.

In evaluation step is applied a method to determine if the evaluated subset is the best current subset. The most used methods present in the literature are ReliefF, correlation-based feature selection, sequential feature selection, gain-ratio feature selection and information gain measure. These filter methods allow to evaluate the subset without using any classification algorithms using training data characteristics such as distance, dependency, consistency, correlation and information.

There are also other models that can be used in order to evaluate the feature subset such as Wrapper, hybrid and embedded models. Wrapper methods evaluate the feature subsets using a predictive model. These train a new model for each subset and test it on a holdout set. Embedded models intend to combine the filter and wrapper methods advantages allowing the feature selection and classification simultaneously. However the filter methods are preferred due to simpler and faster procedure, efficiency and ability to overcome over-fitting [39].

In order to stop the feature selection process there are some different stopping criterion to determine in which situation must occur: the search is complete, the predefined mininum or maximum number of features is achieved and the addition or removal of any feature worsens the outcome of the best found subset until the moment.

Regarding the validation procedure, this step is based on previous others in order to verify the best feature subset. This process may apply several different classifiers upon a new set of features to measure the classification performance and error rate of the selected feature subset [39].

2.6 Classification

The last step in CAD systems is the classification. Once the features are extracted, a classifier is used to lead to the diagnosis that will determine if it is a benign or malignant lesion. For this step a dataset with benign and malignant lesions is needed regardless of the used classifier.

Before skin lesion classification is important to proceed to a feature normalization due to the possibility of having values in different ranges. A widely used method for this normalization is the z-score transformation [25], which transforms all values in order to be in [0,1] range:

$$z_{i,j} = \frac{(v_{i,j} - \mu_j)/(3\sigma j) + 1}{2} \tag{2.17}$$

where $v_{i,j}$ is the value belonging to the ith image of the jth feature and the μ_j and σ_j are the mean and standard deviation of this feature, respectively. Each feature $z_{i,j}$ is normally distributed and should be in the range [0,1]. However, a mininum percentage could present out of range values that must be truncated to either 0 or 1.

In the literature there are different classification methods to discriminate skin lesions in images such as decision trees [42, 25, 33], artificial neural networks (ANN) [30, 33], support vector machines (SVM) [5, 33], instance-based learning [5, 25], Bayesian learning [33] and several ensemble methods [5, 42].

The decision trees can be easily understood as a tree with several nodes that correspond to each taken decision which breaks down a dataset into smaller and smaller subsets until to reach a leaf node that represents a classification.

In ANNs the connections are established between layers of input and output elements with different associated weights that are adjusted during the learning phase in order to predict the correct class output of the input samples. A widely used ANN architecture is the multilayer perceptron (MLP) that allows more than one layer of processing (hidden layer) and the back-propagation learning algorithm that uses backward and forward processes to adjust the weight values of the connections. These classifiers have some disadvantages related to training time that may be very long depending on training set size.

The associated principle of SVMs is the maximization of the margin around the separating hyperplane using a decision function specified by training samples namely support vectors. Thus, it is possible to separate data according to the defined classes.

One of the simplest types of methods to implement is the instance-based classifiers being k-nearest neighbour a very common algorithm in this type of approach. This method uses a distance function to measure the distance of k-nearest neighbours from different k values.

One of the classifiers that also succeeds in diagnosing the lesions is the Naive Bayes classifier. This algorithm is based on density estimation and uses the Bayes' rule that can be written as [7]:

$$p(w|t_1,...,t_n = \frac{p(t_1,...,t_n|w)p(w)}{p(t_1,...,t_n)} \tag{2.18}$$

where $t_1,...,t_n$ are the independent features and w the dependent class on several features.

The ensemble methods are also adopted in the classification step. This strategy allows to combine the results of different classifiers which improves the accuracy of the obtained results. However, it has a much higher computational complexity than by using a single method. The most widely used algorithms are the Boosted and Bagged Trees and the Random Forest.

The performance of the results obtained by each classifier is very important in classification step, since it translates the final verdict about each lesion analyzed and the result obtained by the classifier may influence the physician's decision to remove or not a dubious lesion. Thus, to evaluate this performance it is used some measures namely accuracy, precision, recall and F-measure

from the confusion matrix of classification using the following equations [45]:

$$Accuracy = \frac{(TP+TN)}{(TP+TN+FP+FN)} \tag{2.19}$$

$$Precision = \frac{TP}{(TP+FP)} \tag{2.20}$$

$$Recall = \frac{TP}{(TP+FN)} \tag{2.21}$$

$$F-measure = \frac{(2*Precision*Recall)}{(Precision+Recall)} \tag{2.22}$$

The obtained result from classifier to each skin lesion image can be divided in: true positive (TP), a melanoma image classified as melanoma; true negative (TN), a benign image classified as benign; false positive (FP), a benign image classified as melanoma and false negative (FN), a melanoma image classified as benign.

Accuracy (equation 2.19) represents the percentage of correctly classified samples. Precision (equation 2.20) is defined by the percentage of samples correctly classified as melanoma in the total number of samples. Recall (equation 2.21) is given by the ratio of the samples correctly classified as melanoma to the total number of samples classified as melanoma. F-measure (equation 2.22) is the harmonic mean of precision and recall.

2.7 Summary

This chapter presents a literature review which was essencial for the development of this project. Section 2.1 intended to understand the general concept of skin lesions, the main characteristics that lead to their differentiation and the techniques used by the physicians. Sections 2.2, 2.3, 2.4, 2.5 and 2.6 were devoted to the presentation of several computational methods to address the main steps of a CAD system. In other words, these sections showed some different approaches in order to achieve the main goal of this thesis.

From the first section it can be retained that there is a great diversity of pigmented skin lesions and that many of them are benign. There are a number of factors that make people more susceptible to skin cancer and although melanoma is not the most frequent one, it has the highest deadly rate. Another important aspect is related to the diagnosis, since the task of distinguishing lesions can be quite complex even for the most experienced dermatologists leading to the unnecessary extraction of a benign lesion or the devaluation of a potentially malignant lesion that can metastasize to other parts of the body causing death to the patient. Therefore it becomes evident the need to

implement a CAD system that allows the distinction of these lesions, decreasing the dependence of the diagnosis on physician's experience and consequently the mortality rate.

The following sections present the methods applied for the implementation of such a system. In the pre-processing step, several filters are used to remove/soften unwanted artifacts present in the image to be studied. The inpainting techniques are also efficient for minimizing the impact of hairs on images since it fills these pixels based on neighboring color information. Regarding segmentation, it is possible to verify that there are several techniques that are well studied and used in the literature, which are divided into different categories namely edge-, thresholding-, region-, active contours and artificial intelligence based methods.

The feature extraction allows to gather characteristics related to the shape, color and texture of the lesions that are fundamental for the diagnosis of the lesions. In section 2.4 it is presented some of the attributes used to characterize the border assymetry and irregularity, the color distribution and the presence of dermoscopic structures in the lesion region that allow the desired differentiation. Still in the context of the attributes, the different steps that constitute a selection process are presented as well as the most used methods for the removal of unnecessary and irrelevant attributes.

Classification, as the final step in this type of systems, allows to achieve the results of the diagnosis obtained automatically. This review describes some of the approaches explored in literature studies such as decision trees, SVMs, artificial neural networks, instance- and Bayes based learning. In order to evaluate the performance of these methods, some quality measures based on the results obtained are still presented.

In conclusion, although there is much literature on automatic classification of lesions, studying the main methods used and its results for each of the CAD system steps, the analysis of temporal alterations of the lesions is still a lack and may have potential in the recognition of malignant lesions. Therefore, this was one of the main motivations that led to this work.

The techniques adopted during the accomplishment of this project in order to reach this main goal are presented in the following chapter.

Chapter 3

Methodology

This chapter presents the adopted methodology during this work in order to address the main goal that allows the feature extraction and classification of pigmented skin lesions according to the observed temporal differences.

This chapter was divided in two main subchapters:

- **Image dataset**, identifying the dataset used in the development of the project, quantifying the number of images of benign and malignant lesions that it contains;
- **Adopted approach**, that covers subsections for each step of the system. This includes the description of the methods and techniques adopted as well as the identification of the parameters used during the development of this work.

3.1 Image dataset

During this work it was used a dataset kindly provided by Dr. Jorge Rozeira. It consists of multiple pairs of images being that each pair is related to the same pigmented skin lesion in two distinct moments of evaluation. For each one there is a diagnosis according to the histopathology evaluation done by the physician that will be used as the ground-truth leading to the possible removal of the lesion.

The images from dataset were acquired using a dermoscope and saved in JPG (a compressed image format). These are 24-bit RGB color images with a resolution of 767x576 pixels. This dataset contains a total of 16 pairs referring to melanomas and 8 pairs to benign lesions. Examples of these paired images are shown in figure 3.1.

3.2 Adopted approach

The goal of this thesis was the analysis of temporal variations in skin lesions that may lead to detection of malignant lesions. Thus, the process involves different steps until the desired results

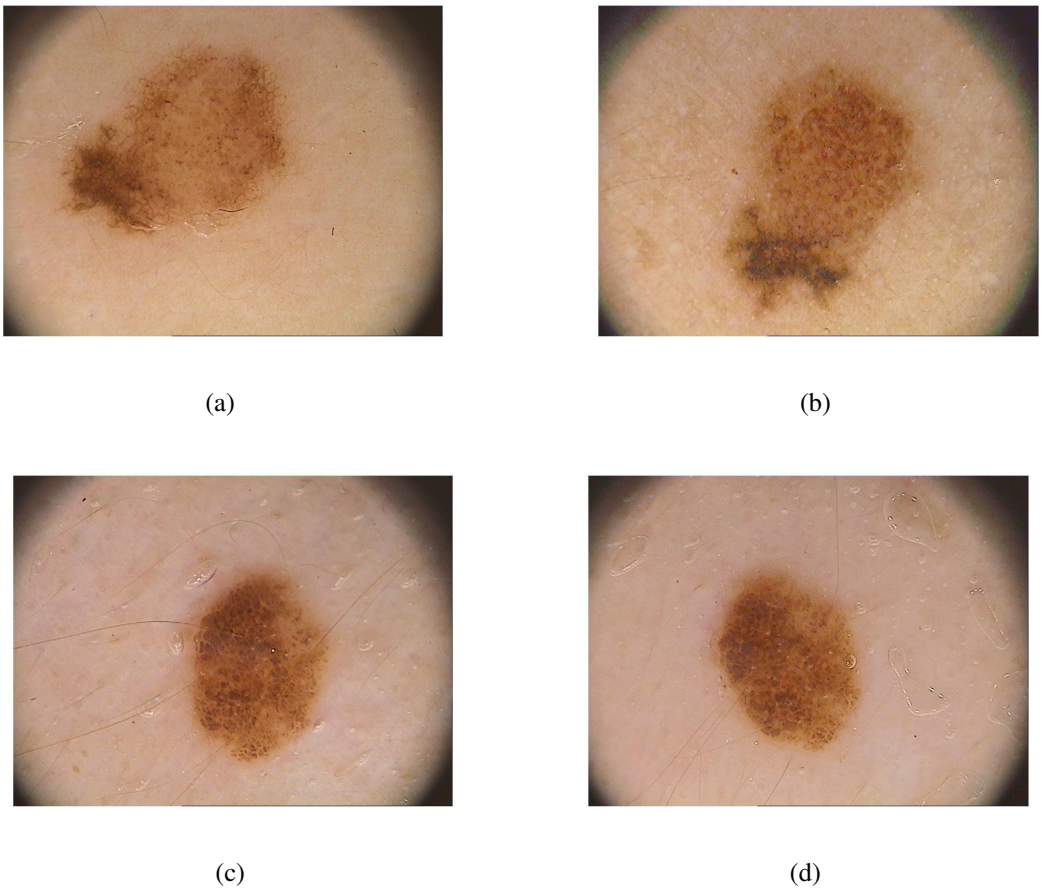

(a) (b)

(c) (d)

Figure 3.1: Two pairs of dermoscopy images from two different lesions: 3.1a and 3.1b refer to the evolution of a malignant lesion; 3.1c and 3.1d refer a benign lesion in two different moments.

namely pre-processing, segmentation, feature extraction, feature selection and classification of each pair of dermoscopy images. In the following subsections are presented the methods adopted for each step.

3.2.1 Pre-processing

The pre-processing step is very important since it prepares the image that will later be segmented in order to improve and evidence the skin lesion from the surrounding healthy skin. In this work the focus was the hair removal attending to its presence in most of the images from the dataset.

For this purpose, an anisotropic filter was applied given the ability to maintain crucial information about lesions, reducing not only the presence of hairs but also smoothing air bubbles, ink marks and other artifacts. Considering the anisotropic diffusion equation 3.1 where *div* indicates the divergence operator, and with ∇ and Δ are respectively the gradient and Laplacian operators, a structure of 8 neighboring nodes was recognized for diffusion conduction and after 15 iterations using $\Delta_t = 1/7$, $K = 30$ and the conduction coefficient function 3.2 that privileges wide regions

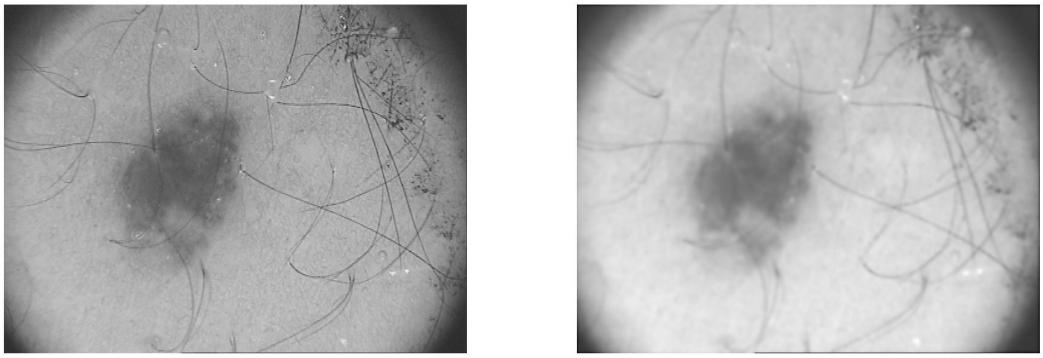

(a) (b)

Figure 3.2: Application of anisotropic diffusion filter: a) original dermoscopy image of a melanoma and b) corresponding image after this filtering.

over smaller ones, the results of the application of this filter introduced by Perona and Malik [40] to the grayscale image are shown in figure 3.2.

$$I_t = div(c(x,y,t)\nabla I) = c(x,y,t)\Delta I + \nabla c \cdot \nabla I \tag{3.1}$$

$$c(\|\nabla I\|) = \frac{1}{1+\left(\frac{\|\nabla I\|}{K}\right)^2} \tag{3.2}$$

Although the application of the above filter has visible effects on the smoothing of such artifacts, it is not sufficient to soften thick hairs. Thus, it was used an approach for the removal of these hairs containing the following steps:

1. production of a binary hair mask by using thresholding where 0 and 1 represents hair and non-hair regions respectively;

2. replacement of hair pixels values by the values of the nearby non-hair pixels using an algorithm based on the Mumford-Shah image model [22].

This inpainting technique focuses on a minimization problem based on Ambrosio and Tortorelli's approximation, equation 3.3, that is solved iteratively via alternating solutions of the Euler-Lagrange equations for u and x.

$$E[z|u] = \frac{\alpha}{2}\int_\Omega z^2|\nabla u|^2 dx + \beta\int_\Omega \left(\varepsilon|\nabla z|^2 + \frac{(1-z)^2}{4\varepsilon}\right) dx \tag{3.3}$$

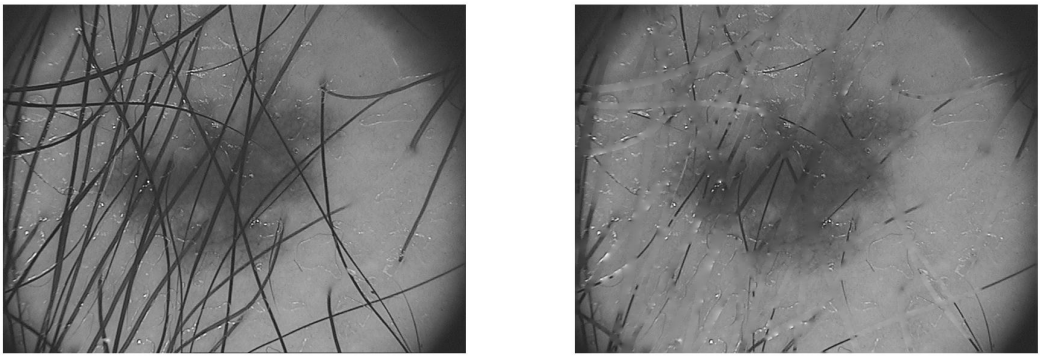

(a) (b)

Figure 3.3: Application of inpainting algorithm: a) original dermoscopy image of a melanoma and b) corresponding image after this technique.

From the parameter values $\gamma = 0.5$, $\varepsilon = 0.05$, $\alpha = 1$ and $\lambda = 1E^9$ and after compute the image gradient and laplacian it is possible to define two differential operators:

$$L_z = -\nabla \cdot z^2 \nabla + \lambda/\gamma \tag{3.4}$$

$$M_u = (1 + 2(\varepsilon\gamma/\alpha)|\nabla u|^2) - 4\varepsilon^2\Delta \tag{3.5}$$

The result of a melanoma RGB image after solving the Euler-Lagrange equations for 40 iterations in each of the 3 channels is shown in figure 3.3.

3.2.2 Segmentation

Segmentation is a crucial process for the correct classification of skin lesions, since it allows to distinguish the lesion from the image, obtaining the ROI that will be studied.

For this work was used the Chan-Vese method that is molded from the Mumford-Shah and level-set segmentation methods. Basically, a curve is deformed toward the lesion edge using a "fitting" term F for the energy minimization. The energy $F(c_1, c_2, \phi)$ that allows to identify whether the ROI is inside or outside the curve can be written as:

$$\begin{aligned} F(c_1,c_2,\phi) = \mu \int_\Omega \delta(\phi(x,y))|\nabla\phi(x,y)|dxdy + \upsilon \int_\Omega H(\phi(x,y))dxdy + \\ \lambda_1 \int_\Omega |u_0(x,y) - c_1|^2 H(\phi(x,y))dxdy + \lambda_2 \int_\Omega |u_0(x,y) - c_2|^2 (1 - H(\phi(x,y)))dxdy \end{aligned} \tag{3.6}$$

where u_0 is a image, μ, $\upsilon \geq 0$, λ_1 and λ_2 are weights for the fitting term and H and δ are the Heaviside and Dirac delta functions. The constants c_1 and c_2 correspond respectively to the

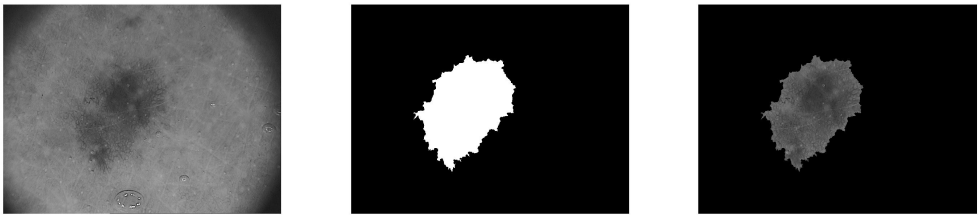

(a) (b) (c)

Figure 3.4: Segmentation of a pigmented skin lesion: a) Original RGB image; b) Binary mask; c) Result of the masking procedure

average (u_0) in $\phi \geq 0$ and in $\phi < 0$ that minimizing energy $F(c_1, c_2, \phi)$. Keeping ϕ these constants are easily expressed by the equation 3.7.

$$c_1(\phi) = \frac{\int_\Omega u_0(x,y)H(\phi(x,y))dxdy}{\int_\Omega H(\phi(x,y))dxdy} \tag{3.7}$$

$$c_2(\phi) = \frac{\int_\Omega u_0(x,y)(1-H(\phi(x,y)))dxdy}{\int_\Omega (1-H(\phi(x,y)))dxdy} \tag{3.8}$$

As a starting point for the segmentation process it is necessary to manually define a binary mask that includes the region of the lesion represented by the 0 values. Through an algorithm that implements the process mentioned above, the region will then converge to the lesion border. The result of segmentation using defined values based on the experimental tests ($\mu = 0.2$, $\lambda_1 = \lambda_2 = 1$) after 350 iterations are shown in figure 3.4.

The binary mask resulting from this process comprises several objects corresponding to a large region (coincident with the lesion) and several others of very small dimensions. In the following steps it will only be considered the object with the greatest area.

3.2.3 Feature extraction

In this step, after the segmentation of the region of interest, the features representing the different properties of the input patterns that help in the differentiation of the skin lesions will be extracted. Thus, the extraction of several features related to the color, shape and texture of the lesions is important for the lesion classification in order to obtain a better final diagnosis, taking into account the changes observed in the lesions over time.

3.2.3.1 Shape features

Shape features intend to describe the lesion through its asymmetry and border irregularity. However, some of these were initially disregarded, since the desired analysis of feature variation required that the images of each pair be congruent in their scale. Given the impossibility to proceed

to the scale transformation, the chosen features present an invariance to the lesion size.

Features such as shape compactness, solidity and rectangularity are easily extracted through the MATLAB *regionprops* function which just requires as input the lesion binary mask obtained in the segmentation step and the name of the desired property. Shape compactness measures the relation between the lesion area to the area of a circle with the same perimeter and is computed using equation 2.1. The value of this measure ranges from 0 to 1 with 1 corresponding a perfect circle, thus melanomas are associated with lower values given their tendency to irregular shapes, unlike the most common nevus which present a regular and circular shape.

Solidity is defined by the ratio between the area of the lesion and its convex hull, which is the region of the smallest convex that encompasses the whole lesion region. As in the case of shape compactness, lower ratios tend to describe melanomas due to the border irregularity given the difference observed between the two areas.

Rectangularity is defined by the ratio of pixels in the region to pixels in the total bounding box (smallest rectangle containing the region) using the height and width parameters of the bounding box. Since melanomas tend to have lower rectangularity values, this may be another good attribute to provide a better differentiation between lesions.

As mentioned in section 2.4.1 the Hu's seven moment-based invariants are also scaling invariant metrics and then possibly to apply during this study. This set of seven moments were calculated using the normalized image moments presented in equations 2.9.

3.2.3.2 Color features

Color also plays an important role in melanoma identification since this type of lesions usually present different colors that may have a uneven distribution. At first it must be proceeded to the image equalization since it will be studied the color alteration between two images of the same lesion. For this, the MATLAB function *histeq* was used in order to enhance the contrast of images by transforming the values in each intensity RGB channel, so that the histogram of the output image approximately matches the histogram of the first, with the maximum and the minimum of each histogram coinciding.

According to section 2.4.2 the RGB color space may not be the best for studying these features. Therefore it has been converted to the HSV color space using the equations presented in 2.10 separating the lightness information from chromaticity.

The color features extracted after the conversion mentioned above were maximum, mininum, mean, standard deviation, skewness and variance of the pixels intensities inside the lesion segment in each channel, following equations 2.12, 2.13, 2.14 and 2.15.

3.2.3.3 Texture features

The physicians look for something that they consider suspicious and indicator of malignancy in the dermoscopy images as it is the case of dots, irregular vascularization, atypical pigment network, structureless areas, among others that is, the analysis of lesion textures. Regardly to the texture features it was employed several descriptors based on second order GLCM.

First, the RGB image have to be converted to grayscale, eliminating the hue and saturation information and keeping the luminance. This transformation is done by giving to each pixel its gray value G following the equation 3.9:

$$G = 0.2989 * R + 0.5870 * G + 0.1140 * B \tag{3.9}$$

In order to obtain a GLCM it was used the MATLAB function *graycomatrix* that includes four parameters that can be specified as: the offset that defines the distance and direction between the pixel-of-interest and its neighbour; the number of levels that determines the size of the GLCM; the gray limits to inform how the values in grayscale image are scaled into gray levels and a boolean to define if the ordering of values in the pixel pairs is considered or not. For this work it was considered 60 gray levels, a distance between pixels of 2 (offset) and symmetrical set to true. The following features were computed in four directions (0^o, 45^o, 90^o and 135^o) in order to be rotation invariant.

The first step to texture feature extraction is the GLCM normalization, which is the division of the number of the counts of each transition $c_{i,j}$ by the total number of transitions N and it is given by the equation 3.10:

$$P_{i,j} = \frac{c_{i,j}}{\sum_{i,j=1}^{N} c_{i,j}} \tag{3.10}$$

where i and j represent respectively the row and column of the matrix.

After normalization four features were extracted namely contrast, correlation, energy and homogeneity, using the following equations:

$$Contrast = \sum_{i,j=1}^{N} P_{i,j}(i-j)^2 \tag{3.11}$$

$$Correlation = \sum_{i,j=1}^{N} P_{i,j} \frac{(i-\mu_i)(j-\mu_j)}{\sigma^2} \tag{3.12}$$

$$Energy = \sqrt{\sum_{i,j=1}^{N} (P_{i,j})^2} \tag{3.13}$$

$$Homogeneity = \sum_{i,j=1}^{N} (P_{i,j})^2 \tag{3.14}$$

For the classification step will be used the average and the range of each feature across the four directions.

3.2.4 Feature selection

Although it is expected that all features contribute significantly to the classification of the lesions, it is more likely that many of them contain redundant or unnecessary information for this process. Therefore this step is very important to facilitate classification, reducing the amount of features used and thus the time required for the process and improving performance by excluding features that have no potential to distinguish the lesions.

For this work Relief algorithm and the Pearson's Correlation Attribute were employed. A description of each will be given below:

- ReliefF Algorithm - This algorithm is an improvement of the relief algorithm and is based on the location of the nearest neighbor of the example that is randomly and iteratively chosen from the data using a distance measure $d()$. According to [47] after the sampling process the score S_i given to each feature i is given by the equation 3.15:

$$S_i = \frac{1}{2}\sum_{k=1}^{l} d(X_{ik} - X_{iM_k}) - d(X_{ik} - X_{iH_k}) \tag{3.15}$$

  where M_k corresponds to the values of feature i for the nearest neighbours to X_k with the same class label and H_k corresponds to the values of the same feature for the nearest neighbours to X_k with different class labels. In order to handle multi-class problem, this equation was expanded to smooth noise effects introducing the probability of the instance from each class. In this work the value of k in implementation was 10.

- Pearson's Correlation Attribute - This method is used to measure the correlation between an attribute and its class label that is how well both are related. This measure can be calculated dividing the covariance between both variables by the square-root of the product of the variance of each one that is given by equation 3.16:

$$\rho_i = \frac{\sum_{k=1}^{m}(x_{k,i} - \bar{x_i})(y_k - \bar{y})}{\sqrt{\sum_{k=1}^{m}(x_{k,i} - \bar{x_i})^2} \cdot \sqrt{\sum_{k=1}^{m}(y_k - \bar{y})^2}} \tag{3.16}$$

  where $x_{k,i}$ represents the value of feature i from sample k and y_k the label of sample k. $\bar{x_i}$ and $\bar{y}$ correspond respectively to the feature i mean and analogously for $\bar{y}$.

The obtained values may vary between -1 and 1 with 1 being the perfect positive correlation, 0 no correlation and -1 the perfect negative correlation.

3.2.5 Classification

The last step to achieve the main goal of this work is the classification. Once the classification is reached, a diagnosis will be made (malignant or benign) taking into account the temporal evolution of the features extracted from the lesion.

Since the extracted features may contain values in different ranges, they were normalized due to the higher efficiency of classifiers for normalized feature values. Based on the mean and standard deviation it is possible to do this scaling using z-score transformation (equation 2.17).

The classification step requires the definition of training sets that usually applies cross-validation or holdout classification methodologies. In cross-validation method the samples are iterativly divided into S portions and S-1 portions are used for training data while remaining is used for testing, until all the samples have been evaluated. The holdout validation selects randomly samples from each class (benign or malignant) and uses that part for training and the remaining for testing. In this work was applied cross-validation.

There are several different classification methods that can be applied after the feature normalization and the training samples selection steps. In this work SVM, KNN and Naive Bayes algorithms are applied in order to classify the pigmented skin lesions.

According to what was presented in the literature review chapter the SVMs have a functioning based on the application of statistical learning to build a hyperplane to distinguish between lesions. This method is widely used since it allows quite general properties. For the implementation of this method a MATLAB function *fitcsvm* was used in order to train data for binary classification (malignant or benign) on predictor data set since it is indicated for low-dimensional datasets. The radial basis function (RBF) was chosen in this function options due to its stability. Using 10-fold cross validation, the code goes through the following steps:

1. Data division into 10 equal size random sets;
2. Training of an SVM classifier on nine of the sets;
3. 10 repetition of first and second steps using one partition each time and training on the other nine partitions;
4. Combination of statistics for each feature.

The KNN algorithm uses a distance metric to measure distance of a number of neighbours in order to classify the lesions. This algorithm was also implemented in MATLAB using *fitcknn* function. The MATLAB *crossval* function was also used to create this classification model. In order to predict the classification of a new point x_{new} this method uses a procedure that finds the number of neighbour of points in the training set X that are nearest to x_{new} and the number of neighbours of response values y to those nearest points and finally assigns the classification label y_{new} that has smallest expected misclassification cost among the values in y. The used distance metric was the Euclidean distance and the number of neighbors was set to 5.

Finally it was used the Naives Bayes algorithm that estimates the predictor densities within each class and according to the Bayes' rule 2.18 and models the posterior probabilities. Then in

order to assign each instance from predictor data it estimates the posterior probability for each class and chooses the one that yelds the maximum probability.

3.3 Summary

In this chapter all the computational methods adopted in this work were described. During the development of this project these techniques were implemented in the MATLAB software, a well-known tool widely used as a FEUP student.

In the pre-processing step an anisotropic filter was applied in order to smooth the image and the thick hairs were partially removed by implementing an inpainting technique. In order to extract the ROI that allows defining the area of the lesion for study it was used the Chan-Vese method.

After these steps, a group of different features related to shape, color and texture were extracted from the ROI in order to help in differentiation of skin lesions. The features are further selected by applying two different methods that measure the potential of the attribute in discriminating a given class.

The resulting features were used in classification step aiming a final diagnosis. These values had to be normalized in order to ensure that they are all in the same range. For the classification purpose were applied three distinct classifiers using 10-fold cross-validation: SVM, KNN and Naive Bayes.

The following chapter presents the obtained results using the previously methods and their analysis.

Chapter 4

Results and Discussion

This chapter presents the results of the work developed and the inherent discussion of them. Firstly, the features resulting from the selection process will be introduced, which will be used in the classification step and then the performance of the classification will be presented.

It should be noted that the algorithms used in the feature selection and classification were applied to the 24 pairs of images of the dataset provided. The three scenarios studied are presented with the following approach:

1. Temporal variations - will be considered the differences in the characteristics of the images for the two distinct moments of evaluation;

2. Second moment evaluation - the characteristics of the lesion will only be considered at the second moment of evaluation;

3. Temporal variations + Second moment evaluation - approach that allows to take into account both the observed differences and the state of the lesion in the second evaluation.

In order to facilitate the understanding of the results, the following acronyms were used for each feature:

In order to distinguish between the variation observed in the features and the features extracted from the second evaluation moment, a "v" will be added to each acronym of the first one. Example: xHuev (difference observed in the mean value of Hue between each evaluation instande).

4.1 Feature selection

In order to choose the most relevant features for the classification of the lesions, two methods were considered: the ReliefF algorithm and the Correlation-based evaluation. The results obtained from feature selection by these methods are partial listed in order of relevance in the table 4.2.

The shape features allow to provide a knowledge regarding the asymmetry and irregularity of the edges of the lesion. However, it can be seen from the table above that this type of feature

Table 4.1: Features Acronyms

Shape Features	Color Features	Texture Features
1^{st} Hu's invariant moment - Hu1	Average H - xHue	Average of Contrast - xCont
2^{nd} Hu's invariant moment - Hu2	Average S - xSat	Range of Contrast - rCont
3^{rd} Hu's invariant moment - Hu3	Average V - xVal	Average of Correlation - xCorr
4^{th} Hu's invariant moment - Hu4	Standard deviation in H - stdHue	Range of Correlation - rCorr
5^{th} Hu's invariant moment - Hu5	Standard deviation in S - stdSat	Average of Energy - xEne
6^{th} Hu's invariant moment - Hu7	Standard deviation in V - stdVal	Range of Energy - rEne
7^{th} Hu's invariant moment - Hu8		Average of Homogeneity - xHom
Compactness - C		Range of Homogeneity - rHom
Rectangularity - R		
Solidity - S		
Perimeter/Area Ratio - Pa		

does not figure in a good ranking position (the best shape feature appears in the third position in the better of cases). This means that these characteristics are not the best to predict whether the lesions are malignant or not. In fact, malignant lesions often do not present or tend to become more irregular over time as shown in figure 4.1, just as the benign lesions sometimes have and tend to have more asymmetric borders.

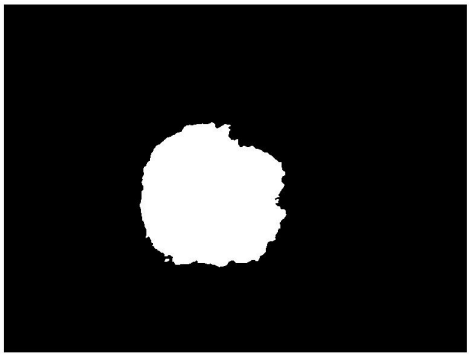

Figure 4.1: Binary image of a malignant lesion segmentation

Another aspect that negatively influences the ranking position of this type of features are the presence of hairs in several images. Although an effort is made to attenuate the unwanted factors such as hairs, air bubbles and ink marks with the application of an anisotropic filter and an in-painting algorithm, the hairs are still visible in many cases, especially when it comes to lesions in regions of the body with great density of thick hairs. After the pre-processing step the result of the segmentation may be similar to the figure 4.2.

Thus, it is possible to conclude that although shape descriptors may contain important information in many cases, they are often considered irrelevant to the classification process due to the inherent weakness of segmentation and the existence of malignant lesions with benign similarities,

Table 4.2: Partial ranking of features according to the Pearson's Coefficient Attribute and the ReliefF algorithm for three different scenarios

Ranking	Scenario					
	1		2		3	
	Feature	Score	Feature	Score	Feature	Score
1	stdHuev	0.022213	rCont	0.011716	stdHuev	0.02094
2	xHuev	0.01621	rCorr	0.01119	stdHue	0.02094
3	rEnerv	0.006102	Hu4	0.00816	xHuev	0.01783
4	rHomov	0.003549	C	0.005633	rEnerv	0.01619
5	xValv	-0.000669	Hu2	0.005407	Hu4	0.01364
6	Cv	-0.000817	xHue	0.003533	Hu2	0.01257
7	xEnerv	-0.00155	E	0.001904	xHue	0.00849
8	Ev	-0.006079	S	0.000135	rHomov	0.00713
9	Pv	-0.008614	rHomo	-0.001217	rCorr	0.00633
10	stdValv	-0.009636	xHomo	-0.002006	rCont	0.0047
11	xSatv	-0.011947	xSat	-0.004467	rHomo	0.00349
12	Hu1v	-0.012956	stdHue	-0.004706	xSat	-0.00236
13	stdSatv	-0.014109	stdSat	-0.008147	xEnerv	-0.00304

with tendentially circular shapes and/or symmetrical and regular edges.

As mentioned in the literature review section, color features are quite important for the differentiation of lesions and considered in different diagnostic methods. In this work these features are extracted from the converted RGB image into HSV model regarding the average and standard deviation of lesion saturation, hue and value.

As can be seen in the table **??**, this type of descriptors are the most relevant when using ReliefF algorithm and therefore are the best predictors in distinguishing the type of lesion specially when taking in account the temporal variations. The measures of the hue average and the hue standard deviation are clearly the best ones in that cases. Figure 4.3 illustrates most of the malignant lesions of the studied dataset having distinct color regions, temporal alterations from light to dark brown and areas of poor pigmentation.

The extraction of texture features also supports the diagnoses made by dermatologists since they contain information that may indicate malignancy such as an atypical pigment network and structureless areas. This type of descriptors are evidently the best predictors from this feature selection step. These figure in the first two places using Pearson's correlation attribute in all the scenarios and still using the ReliefF algorithm when applied to the attributes in the second moment of evaluation. Figure 4.4 shows a dermoscopy image of a malignant lesion where an atypical pigment network and certain structureless areas are clearly visible. These characteristics are fundamental for the differentiation of lesions, given their level of evidence in almost all images that refer to malignant lesions.

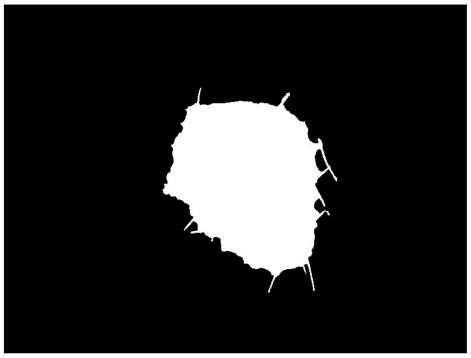

Figure 4.2: Binary image of a benign lesion segmentation with visible influence of hairs

It is also interesting to conclude from the table that for the third scenario (Temporal variations + Second Moment Evaluation) the features in the ranking are mostly those that refer to the temporal variation of each lesion and not only to the second evaluation. When using the PCA the feature set presented only refers to these alterations.

4.2 Prediction performance

After analyzing the best features according to the previous ranking selected by the two methods in each of the situations, three classifiers will be considered in order to compare and evaluate the prediction performance namely KNN, SVM, and Naive Bayes.

During this process 8-fold cross-validation is used on the training data, that is the original data is randomly partitioned into 8 equal sized subsamples being a single one retained as the validation data and the remaining used as training data.

The accuracy results of each classifier, taking into account the selected features by the Relieff algorithm and Pearson's correlation attribute (PCA) are presented in the table 4.3 for each of the three scenarios studied.

Table 4.3: Classification accuracy using the selected features for three different scenarios

Method	ReliefF			PCA		
	Scenario			Scenario		
	1	2	3	1	2	3
KNN [%]	66.7	54.2	58.3	66.7	41.7	62.5
SVM [%]	62.5	54.2	50.0	62.5	58.3	50.0
Naïve Bayes [%]	41.7	16.7	41.7	37.5	20.8	37.5

From the observation of the table **??** is possible to recognize that the obtained results are not the expected ones. The second scenario presents the worst results in almost all the studied cases, only

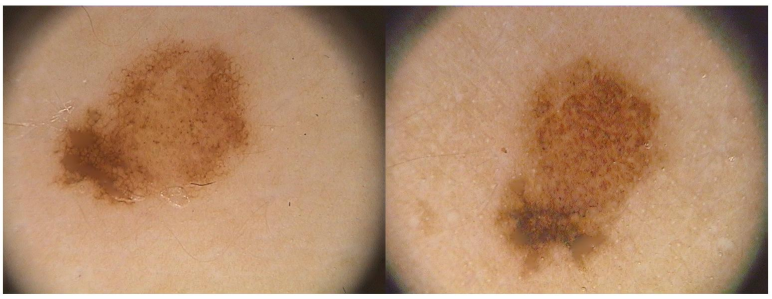

Figure 4.3: Temporal alterations of a malignant lesion

surpassing the third scenario when using the SVM classifier. This means that the classification is not generally effective taking into account only the characteristics of an image.

For both selection algorithms is also possible to notice that the higher accuracy is always related to the first scenario, thus confirming the potentiality of the analysis of temporal variations of the features in classification of the skin lesions. The highest achieved result in accuracy is 66.7% using KNN classifier.

In order to better exploit the results, table 4.4 shows some of the performance measures of the classifier calculated from the confusion matrix.

Table 4.4: Performance measures calculated from each confusion matrix related to the three scenarios studied [%]

Scenario	Feature Selection	Classification	Accuracy	Precision	Recall	F-measure
1	ReliefF	SVM	62.5	65.2	93.8	76.9
1	PCA	SVM	62.5	65.2	93.8	76.9
1	ReliefF	KNN	66.7	66.7	100	80.0
1	PCA	KNN	66.7	66.7	100	80.0
1	ReliefF	NB	41.7	56.3	56.3	56.3
1	PCA	NB	37.5	52.9	56.3	54.5
2	ReliefF	SVM	54.2	61.9	81.3	70.3
2	PCA	SVM	58.3	63.4	87.5	73.5
2	ReliefF	KNN	54.2	61.9	81.3	70.3
2	PCA	KNN	41.7	55.6	62.5	58.8
2	ReliefF	NB	16.7	30.0	18.8	23.1
2	PCA	NB	20.8	38.5	31.3	34.5
3	ReliefF	SVM	50.0	58.8	66.7	64.0
3	PCA	SVM	50.0	57.9	73.3	64.7
3	ReliefF	KNN	58.3	60.9	93.3	73.7
3	PCA	KNN	62.5	62.5	100	76.9
3	ReliefF	NB	41.7	57.1	50.0	53.3
3	PCA	NB	37.5	52.9	56.3	54.5

From the table 4.4 it can be seen that the percentage of precision and recall are slightly higher

Figure 4.4: Dermoscopy image of a malignant lesion with an atypical pigment network

than the accuracy showing that although the number of correct classifications is not high, the performance in malignant lesions classification is higher and the percentage of correctly classified melanomas in the total number of samples classified as melanoma is even better.

In fact, in the case of applying this diagnosis to a patient is preferable to have false positives than false negatives, such as the obtained results, because a benign lesion classified as melanoma has only the drawback of unnecessary removal of that lesion but a malignant classified as a benign one can be ignored, progressing and metastasizing to the whole body.

However, the goal is always to develop an increasingly reliable system therefore it is expected that the values of accuracy will be as high as possible. The low accuracy and precision results may be related to the low dimension of the dataset studied. In fact, the task of getting these images is quite difficult. This is in part due to the precaution of physicians in removing the lesions that are doubtful. Therefore, there are few cases where a potentially malignant lesion is monitored over time. Only some lesions need vigilance because when firstly evaluated they do not have any malignant prediction.

Another fundamental aspect is the constitution of the dataset. The fact that the distribution of images is not balanced with a ratio of two thirds belonging to the malignant lesions set (16) and only one third for benign lesions images (8) makes the classification tend to be better for malignant lesions. In summary, the lack of true negatives, that is, benign lesions classified as such, is due in part to the poor information regarding this type of lesions, resulting in low values for accuracy. Therefore an improvement may be possible for these results with a balanced distribution including in the dataset the same number of images for each class.

4.3 Computational time

In the proposed approach all the algorithms were implemented using MATLAB R2017b environment on an Intel(R) Core(TM) i7-4810MQ CPU @ 2.80GHz with 16 GB of RAM running Windows 10 Pro 64-bits. Table 4.5 shows the computational time of processing each image for each

task, including the anistropic filter application, the inpainting technique, the lesion segmentation, the extraction of shape, texture and color features and the classification using the best method.

Table 4.5: Computational time for this work tasks considering each image

Task	Features	Time (s)
Anisotropic filter		0.6112
Inpainting algorithm		169.0372
Segmentation		34.3805
Shape feature extraction	11	1.9201
Texture feature extraction	8	0.3861
Color feature extraction	6	0.0354
Classification	44	0.65
Total		207.0205

These values show that the pre-processing step was the most time consuming task. It can also be concluded that the computation of the feature measures based on shape, color and texture characteristics and the classification are relatively fast processes. It is important to note that each of these tasks is performed for each pair of images. The processing of all the images is then a very time consuming task needing about three hours.

4.4 Summary

The achieved results are explained throughout this chapter. It were used two different feature ranking methods in order to select the best features and were evaluated the perfomance of three classifiers.

The feature selection concluded that texture and color features showed consistency related to the predictive value between the studied scenarios. In fact the images present in the dataset have high resolution allowing the color and the structure information from the image be crucial for the characterization of the lesions.

The shape descriptors do not figure in the top of ranking, in part due to the influence of segmentation step. The hairs commonly presented in the studied dataset are attenuated during the pre-processing step but is not always an effective procedure when it comes to thick hairs, resulting in a segmentation influenced by them. Thus the detection of the edges becomes more difficult, being often misrepresented due to the hairs.

Regarding the performance of the classifiers, the best accuracy results were achieved using the KNN classifier for the first scenario. This analysis allows to conclude that there is a slight improvement of the classification using the first scenario. In other words, the use of feature variation between two time intervals presents a more accurate classification than using only the current characteristics of the lesion.

For the results of precision, recall and f-measure there are some improvements observed, allowing to conclude that the efficacy of the classification of melanomas is greater than in terms of differentiation between lesions. It is believed that better results would be achieved with a larger and a balanced dataset, with the same number of pairs of malignant and benign lesions.

Finally, a table with the computational duration of each task is presented, which shows that the processing of all these images was a slow and complex work.

Chapter 5

Conclusions and Future Work

5.1 Final conclusions

CAD systems are the subject of several studies to assist physicians in the diagnosis of pigmented skin lesions. The goal is to increasingly ensure a reliable process for the differentiation of malignant and benign lesions. Based on different color, shape and texture characteristics extracted from the dermoscopic images a classification will be made. However, the lack of developed studies that perform this process based on the temporal alteration of the lesions is noticed, ignoring the development of its appearance over time.

With the analysis of temporal variations as the main motivation for this project, an approach was presented that allowed the classification of skin lesions from the dermoscopy images dataset kindly provided by Dr. Jorge Rozeira. This work has covered the common CAD system steps namely pre-processing, segmentation, feature extraction, feature selection and classification.

In the pre-processing step were employed an anisotropic filter to smooth the image and an inpainting algorithm to remove most of the thick hairs. The resulted images after the application of these techniques proved to be interesting due to the attenuation of unwanted factors such as hairs, air bubbles and ink marks that could affect the following step.

In the extraction of the ROI was used the proposed model by Chan and Vese as the segmentation method. In order to perform this process, a polygon was manually defined outside lesion area that applying this algorithm it was iteratively deformed toward the lesion edge. The obtained result presented as a binary mask may contain several objects but only the larger area one was considered for the next steps.

The different lesion characteristics may be evidenced with the feature extraction step. During this procedure 11 shape features, 8 texture features and 6 color features were extracted in order to differenciate the lesions. The selection of the main predictive attributes was performed using the ReliefF algorithm and the Pearson's correlation attribute for each of the three distinct scenarios:

1. Analysis of temporal variations in pigmented skin lesions;

2. Lesion analysis in the second moment of evaluation;

3. Analysis of temporal variations and the second moment lesion evaluation.

Later these scenarios allowed to evaluate the effectiveness of a system based on the evolution of the lesions. The texture and color features proved to be fundamental for the classification of the lesions, which may be related to the high resolution of the used images. On the other hand, shape features did not appear in the top of this ranking probably due to the influence of some thick hairs in the segmentation results.

Classification is the last step to achieve the main purpose of a CAD system that defines a final diagnosis. For each of the cases previously explained, three classifiers were applied using 8 fold cross validation: the SVM, the KNN and the Naive Bayes algorithms.

The obtained accuracy and precision results allow to conclude that there is an effective improvement in the classification when taking into account the temporal variations of the lesion. In all cases, scenario 1 presents better results than scenario 2. Scenario 3 presents better performance than 2 but still does not exceed the values obtained only with the variation observed in the features. However, the number of considered features for the study of the third scenario is twice as high as those considered in 1 and 2. As in the other scenarios only 13 features were selected and used which may explain slightly lower values.

Another of the identified problems that can explain these values is constitution of the used dataset. Apart from the dimension not large enough to achieve more precise results, the number of malignant and benign lesions is also quite different. This resulted in the almost nonexistence of false positives, that is, benign lesions classified as benign. Thus, although satisfactory results have been achieved related to the classification of malignant lesions, according to this system many benign lesions may be unnecessarily extracted.

5.2 Future work

Since the results prove the potentiality of the analysis of the evolution of the lesions it is believed that considering a larger, balanced and more diverse used dataset would improve the obtained accuracy values.

It might also be interesting to achieve satisfactory results using this kind of approach in macroscopic images obtained using common digital cameras. It is clear that the evaluation by a physician is indispensable for the diagnosis but in this case, any patient could self-evaluate the lesions that they considered potentially malignant.

Other methods for the segmentation, feature selection and classification steps must be studied in order to evaluate the performance of each one improving the diagnostic accuracy of the CAD systems in dermatology.

Bibliography

[1] *Advanced Biomedical Image Analysis*, chapter 9. •, 2010.

[2] Qaisar Abbas, M. Emre Celebi, and Irene Fondón. A novel perceptually-oriented approach for skin tumor segmentation. Vol 8:1837–1848, 04 2012.

[3] Marwan Al-Akaidi. *Fractal Speech Processing*. Cambridge University Press, New York, NY, USA, 2004.

[4] Giuseppe Argenziano, Gabriella Fabbrocini, Paolo Carli, Vincenzo De Giorgi, Elena Sammarco, and Mario Delfino. Epiluminescence microscopy for the diagnosis of doubtful melanocytic skin lesions. 134, 12 1998.

[5] C. Barata, M. Ruela, M. Francisco, T. Mendonça, and J. S. Marques. Two systems for the detection of melanomas in dermoscopy images using texture and color features. *IEEE Systems Journal*, 8(3):965–979, Sept 2014.

[6] C.A.Z. Barcelos and V.B. Pires. An automatic based nonlinear diffusion equations scheme for skin lesion segmentation. *Applied Mathematics and Computation*, 215(1):251 – 261, 2009.

[7] Christopher M. Bishop. *Pattern Recognition and Machine Learning (Information Science and Statistics)*. Springer-Verlag, Berlin, Heidelberg, 2006.

[8] Ralph Peter Braun, Harold S. Rabinovitz, Margaret Oliviero, Alfred W. Kopf, and Jean-Hilaire Saurat. Dermoscopy of pigmented skin lesions. *Journal of the American Academy of Dermatology*, 2005.

[9] J. Canny. A computational approach to edge detection. *IEEE Transactions on Pattern Analysis and Machine Intelligence*, PAMI-8(6):679–698, Nov 1986.

[10] Francine Catté, Pierre-Louis Lions, Jean-Michel Morel, and Tomeu Coll. Image selective smoothing and edge detection by nonlinear diffusion. *SIAM Journal on Numerical Analysis*, 29(1):182–193, 1992.

[11] Pablo G. Cavalcanti and Jacob Scharcanski. *Macroscopic Pigmented Skin Lesion Segmentation and Its Influence on Lesion Classification and Diagnosis*, pages 15–39. Springer Netherlands, Dordrecht, 2013.

[12] M. E. Celebi, Y. A. Aslandogan, and P. R. Bergstresser. Unsupervised border detection of skin lesion images. In *International Conference on Information Technology: Coding and Computing (ITCC'05) - Volume II*, volume 2, pages 123–128 Vol. 2, April 2005.

[13] M. E. Celebi, G. Schaefer, H. Iyatomi, and W. V. Stoecker. Lesion border detection in dermoscopy images. *Comput Med Imaging Graph*, 2009.

[14] M. Emre Celebi, Y Alp Aslandogan, William Stoecker, Hitoshi Iyatomi, Hiroshi Oka, and Xiaohe Chen. Unsupervised border detection in dermoscopy images. 13:454–62, 12 2007.

[15] M. Emre Celebi, Hassan Kingravi, Hitoshi Iyatomi, Y Alp Aslandogan, William Stoecker, Randy Moss, Joseph M Malters, James Grichnik, Ashfaq A Marghoob, Harold S Rabinovitz, and Scott W Menzies. Border detection in dermoscopy images using statistical region merging. 14:347–53, 09 2008.

[16] M. Emre Celebi, Hassan Kingravi, Bakhtiyar Uddin, Hitoshi Iyatomi, Y Alp Aslandogan, William Stoecker, and Randy Moss. A methodological approach to the classification of dermoscopy images. 31:362–73, 10 2007.

[17] M. Emre Celebi, Quan Wen, Sae Hwang, Hitoshi Iyatomi, and Gerald Schaefer. Lesion border detection in dermoscopy images using ensembles of thresholding methods. 19, 06 2012.

[18] F. S. Cohen, Z. Fan, and S. Attali. Automated inspection of textile fabrics using textural models. *IEEE Transactions on Pattern Analysis and Machine Intelligence*, 13(8):803–808, Aug 1991.

[19] M. Dash and H. Liu. Feature selection for classification. *Intelligent Data Analysis*, 1(1):131 – 156, 1997.

[20] H. de Souza Ganzeli, J. Godoy Bottesini, L. de Oliveira Paz, and M. Figueiredo Salgado Ribeiro. Skan: Skin scanner - system for skin cancer detection using adaptive techniques. *IEEE Latin America Transactions*, 9(2):206–212, April 2011.

[21] Mahmoud Elgamal. Automatic skin cancer images classification. *International Journal of Advanced Computer Science and Applications(IJACSA)*, 2013.

[22] Selim Esedoglu. Digital inpainting based on the mumford-shah-euler image model. 13, 08 2003.

[23] P. M. Ferreira, T. Mendonça, J. Rozeira, and P. Rocha. An annotation tool for dermoscopic image segmentation. In *Proceedings of the 1st International Workshop on Visual Interfaces for Ground Truth Collection in Computer Vision Applications*, VIGTA '12, pages 5:1–5:6, New York, NY, USA, 2012. ACM.

[24] Jan Flusser and Tomás Suk. Pattern recognition by affine moment invariants. *Pattern Recognition*, 26(1):167 – 174, 1993.

[25] Pablo G Cavalcanti and Jacob Scharcanski. Automated prescreening of pigmented skin lesions using standard cameras. 35:481–91, 04 2011.

[26] Fei Gao and Pengcheng Shi. *Shape Analysis in Molecular Imaging*, pages 51–93. Springer International Publishing, Cham, 2014.

[27] R. M. Haralick, K. Shanmugam, and I. Dinstein. Textural features for image classification. *IEEE Transactions on Systems, Man, and Cybernetics*, SMC-3(6):610–621, Nov 1973.

[28] Ming-Kuei Hu. Visual pattern recognition by moment invariants. *IRE Transactions on Information Theory*, 8(2):179–187, February 1962.

[29] Sinan Kockara, Mutlu Mete, and Sait Suer. *Color and Spatial Features Integrated Normalized Distance for Density Based Border Detection in Dermoscopy Images*, pages 41–61. Springer Netherlands, Dordrecht, 2013.

[30] Li Ma and Richard C. Staunton. Analysis of the contour structural irregularity of skin lesions using wavelet decomposition. *Pattern Recognition*, 46(1):98 – 106, 2013.

[31] Zhen Ma and Joao Tavares. A novel approach to segment skin lesions in dermoscopic images based on a deformable model. 20:615–623, 03 2016.

[32] Zhen Ma and João Manuel R.S. Tavares. Effective features to classify skin lesions in dermoscopic images. *Expert Systems with Applications*, 84:92 – 101, 2017.

[33] I. Maglogiannis and C. N. Doukas. Overview of advanced computer vision systems for skin lesions characterization. *IEEE Transactions on Information Technology in Biomedicine*, 13(5):721–733, Sept 2009.

[34] J.B.Antoine Maintz and Max A. Viergever. A survey of medical image registration. *Medical Image Analysis*, 2(1):1 – 36, 1998.

[35] Jianchang Mao and Anil K. Jain. Texture classification and segmentation using multiresolution simultaneous autoregressive models. 25:173–188, 02 1992.

[36] M. Messadi, A. Bessaid, and A. Taleb-Ahmed. Extraction of specific parameters for skin tumour classification. *Journal of Medical Engineering & Technology*, 33(4):288–295, 2009. PMID: 19384704.

[37] Hengameh Mirzaalian, Tim Lee, and Ghassan Hamarneh. Skin lesion tracking using structured graphical models. 27, 04 2015.

[38] Francisco Oliveira and Joao Tavares. Medical image registration: A review. 17:73–93, 01 2014.

[39] Roberta B. Oliveira, Aledir S. Pereira, and João Manuel R. S. Tavares. Computational diagnosis of skin lesions from dermoscopic images using combined features. *Neural Computing and Applications*, Mar 2018.

[40] P. Perona and J. Malik. Scale-space and edge detection using anisotropic diffusion. *IEEE Transactions on Pattern Analysis and Machine Intelligence*, 12(7):629–639, Jul 1990.

[41] P. Shanmugavadivu and V. Sivakumar. Fractal dimension based texture analysis of digital images. *Procedia Engineering*, 38:2981 – 2986, 2012. INTERNATIONAL CONFERENCE ON MODELLING OPTIMIZATION AND COMPUTING.

[42] Bijaya Shrestha, Joseph Bishop, Keong Kam, Xiaohe Chen, Randy Moss, William Stoecker, S.E. Umbaugh, Ronald Stanley, M. Emre Celebi, Ashfaq A Marghoob, Giuseppe Argenziano, and Peter Soyer. Detection of atypical texture features in early malignant melanoma. 16:60–5, 02 2010.

[43] M. Silveira, J. C. Nascimento, J. S. Marques, A. R. S. Marcal, T. Mendonca, S. Yamauchi, J. Maeda, and J. Rozeira. Comparison of segmentation methods for melanoma diagnosis in dermoscopy images. *IEEE Journal of Selected Topics in Signal Processing*, 3(1):35–45, Feb 2009.

[44] American Cancer Society. Key statistics for melanoma skin cancer, 2018.

[45] R. Sumithra, Mahamad Suhil, and D.S. Guru. Segmentation and classification of skin lesions for disease diagnosis. *Procedia Computer Science*, 45:76 – 85, 2015. International Conference on Advanced Computing Technologies and Applications (ICACTA).

[46] Suresh. Dermoscopic image segmentation using machine learning algorithm. 8:1159–1168, 11 2011.

[47] Jiliang Tang, Salem Alelyani, and Huan Liu. Feature selection for classification: A review.

[48] M. Tkalcic and J. F. Tasic. Colour spaces: perceptual, historical and applicational background. In *The IEEE Region 8 EUROCON 2003. Computer as a Tool.*, volume 1, pages 304–308 vol.1, Sept 2003.

[49] S W Menzies, C Ingvar, and W H McCarthy. A sensitivity and specificity analysis of the surface microscopy features of invasive melanoma. 6:55–62, 03 1996.

[50] Xianghua Xie. A review of recent advances in surface defect detection using texture analysis techniques. 7, 01 2008.

[51] Z. Xie and G. E. Farin. Image registration using hierarchical b-splines. *IEEE Transactions on Visualization and Computer Graphics*, 10(1):85–94, Jan 2004.

[52] Chenyang Xu and J. L. Prince. Snakes, shapes, and gradient vector flow. *IEEE Transactions on Image Processing*, 7(3):359–369, Mar 1998.

[53] H. Zhou, G. Schaefer, M. E. Celebi, H. Iyatomi, K. A. Norton, T. Liu, and F. Lin. Skin lesion segmentation using an improved snake model. In *2010 Annual International Conference of the IEEE Engineering in Medicine and Biology*, pages 1974–1977, Aug 2010.